

FAR-INFRARED OPTICS DESIGN & VERIFICATION

Phase II

Ghassan Yassin¹, Stafford Withington¹, Cr  idhe O’Sullivan²,
J. Anthony Murphy², Willem Jellema³, Paul Wesselius³,
Tully Peacocke⁴ and Bruno Leone⁵

¹Cavendish Laboratory, Madingley Road, Cambridge, UK

²National University of Ireland Maynooth, Co.Kildare, Ireland

³National Institute for Space Research, Groningen, the Netherlands

⁴UK Astronomy Technology Centre, Royal Observatory, Edinburgh, UK

⁵The European Space Agency (ESA), Noordwijk, the Netherlands

Abstract: In this paper we compare the performance of several commercial software packages (GRASP, ASAP, CODE V, GLAD) as well as the Gaussian beam mode method, in analysing the behaviour of submillimetre systems. The study was commissioned by the European Space Agency (ESA) and was carried out in two phases. In **Phase I** we allowed these packages to simulate the behaviour of carefully selected test cases in order to reveal their strengths and weaknesses. In **Phase II** we first investigate the ability of the packages to predict the performance of a whole submillimetre system. We also compare the simulated results with those predicted by near field amplitude and phase measurements.

1. Introduction

At present there is considerable interest in modelling the electromagnetic properties of submillimetre systems. For example, in the area of astronomical instruments, there are ongoing intensive activities to analyse the behaviour of optical systems corresponding to the projects “HARP”, “ALMA” and the ESA missions “HERSCHEL” and “PLANK”. The reasons for this increased effort may be summarised as follows:

- The continuous improvement in receiver technology and fabrication of optical components. This clearly invites comparable progress in the modelling and design tools.
- The availability of commercial software packages which can provide accurate, yet fast, modelling of optical systems at submillimetre wavelengths.
- The increased numerical processing speed of computers, which allows rigorous mathematical procedures to be incorporated into commercial software packages.

Based on this, ESA has launched a programme to investigate the ability of existing verification and design tools to predict the behaviour of quasi-optical systems in the submillimetre and far-infrared regions. The programme was planned in two phases. In **Phase I** we investigated the ability of several well known commercial software

packages to analyse the field scattered by optical components when illuminated by near or far field sources. The software packages that were chosen for this purpose were GLAD, GRASP, CODE V and ASAP. Occasionally, the package ZEMAX was also tested as well as a non-commercial Gaussian mode analysis software which was written by two of the authors. The single-component test cases were carefully selected in order to emphasise the strengths and the weaknesses of each package in providing reliable information which electromagnetically characterises a quasi-optical system. In particular, we wanted to assess the ability of the packages to simulate the following features:

- the near and far field radiation patterns,
- the vector nature of the electromagnetic fields (eg co-polar and cross-polar components),
- rigour versus speed of computation.

Our selected test cases also reflected the fact that we were interested in relating the simulations to the underlying electromagnetic computational method implemented by the packages. This, in many cases, helped us to understand the difficulties that some packages had in simulating common and simple cases. A complete description of the Phase I results have already been reported [1], [2].

The purpose of Phase II of the project is two-fold. After understanding the basic operation of the software packages we want to examine their ability to analyse the behaviour of a real submillimetre system. For this purpose we have chosen one of the HIFI channels of the ESA space telescope *HERSCHEL*. The analysis was carried out in the frequency range 480-640 GHz and focused on the ability of the packages to predict the near field patterns at the image plane of the system. The second major task in Phase II is the construction of a simplified version of the HIFI channel and a near field test system which is capable of measuring both the amplitude and phase of the radiated fields. The specifications of the test system were chosen in order to both compare the performance the packages and to assess the integrity of the best of them against experimental results.

2. Description of the Software Packages

We shall now provide a brief description of the basic operation of the packages mentioned above. Before that however, we would like to emphasise two issues. The first is that this presentation should not be considered as a full description of the package features or capabilities. The second is that since this work was carried out, some packages have either modified main features and/or added new ones. Clearly we are unable to comment on these modifications.

2.1 ASAP (Advanced Systems Analysis Programme): This package employs beam decomposition to form the aperture field distribution. The software samples the aperture either in the spatial domain or in the angular domain. The field distribution is then propagated using Gaussian ray Gaussian tracing. Our simulation results show that the software seems to experience difficulties whenever the scattering aperture is a few wavelengths across. This is to be expected, however, since rigorous analysis requires the full Gabor decomposition method where the Gaussian beams are both

displaced and rotated with respect to each other. To illustrate this point we show in Fig. 1 the computed far field pattern at 480 GHz for an ideal corrugated horn of aperture radius 2.5 mm and length 15.4 mm. The distance between the horn aperture and the plane of observation was 200 mm.

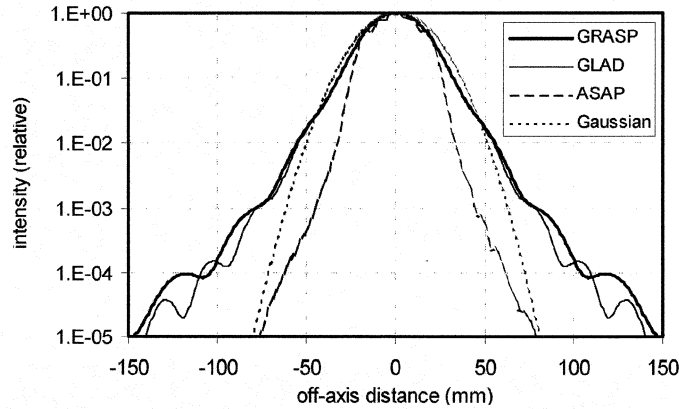


Figure 1. 480-GHz predicted far-field of an ideal corrugated horn of length 15.4mm and aperture radius 2.5mm. The calculations were made by ASAP, GRASP and GLAD and are compared with those of a Gaussian field.

From Fig. 1 it can easily be seen that the pattern calculated by ASAP is substantially narrower than those predicted by the other packages. In fact the results computed by ASAP did not improve even when the pattern was taken at the focal plane of a focusing element.

2.2 CODE V : This package employs both ray tracing and diffraction calculations. It performs Fraunhofer diffraction to calculate the far field and claims to use the angular spectrum method to calculate near fields. Our experience however showed that CODE V tends to have difficulties in producing accurate results in two distinct cases:

- near field diffraction from offset reflectors,
 - far field diffraction when the pattern was viewed in a plane away from focus.
- We shall return to this point when we discuss the analysis of the HERSCHEL HIFI channel.

2.3 GLAD (General Laser Analysis and Design): The principle of operation of this package is based on a plane wave decomposition of the aperture fields [3]. The incident fields are expanded in terms of plane waves and the radiated field is found by integrating over all the spectral components. A two dimensional version of the method is illustrated in Fig.2

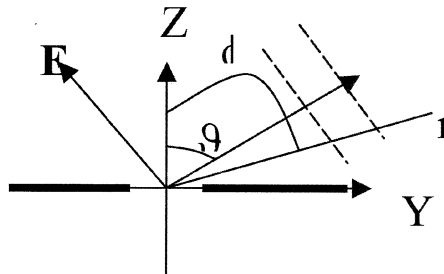


Figure 2 Plane wave decomposition in two dimensions

Here we show an electromagnetic wave illuminating a slit with the electric field in the plane of incidence. The field is therefore expanded for $z > 0$ as:

$$\mathbf{E}(y, z) = \int_{-\pi/2}^{\pi/2} E(\vartheta) [-\cos \vartheta \hat{\mathbf{y}} + \sin \vartheta \hat{\mathbf{z}}] e^{-ik(y \sin \vartheta + z \cos \vartheta)} d\vartheta$$

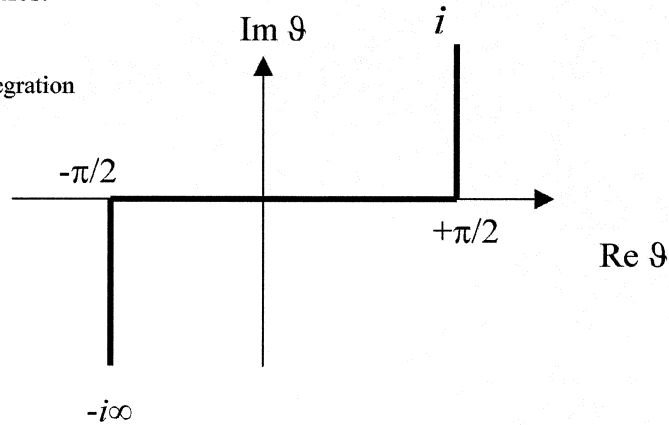
It can then be easily shown that the radiated near field in polar coordinates is given by:

$$\mathbf{E}(r, \phi) = \frac{1}{\lambda} \int_{\infty \mathcal{C}} \left\{ F(k \sin \vartheta) [\cos(\vartheta - \phi) \hat{\phi} + \sin(\vartheta - \phi) \hat{\mathbf{r}}] e^{-ikr \cos(\vartheta - \phi)} \right\} d\vartheta$$

$$F(k_y) = \int_{-\infty}^{\infty} E_y(y, 0) e^{-ik_y y} dy \quad k_y = k \sin \vartheta$$

Similar expressions can be derived for the magnetic field. The contour of integration is shown in Fig. 3 where evanescent waves are also taken into account by integrating over the imaginary axes.

Figure 3 Contour of integration



It is interesting to note that the radiated field has both a longitudinal and transverse component, confirming the near field nature of this treatment. It can be shown that the radial component vanishes as the plane of observation is moved away from the aperture. Plane waves expansion is well known and has been treated by many authors [4]. However since the software package GLAD performed much better in our simulations than was initially anticipated, we list below some important features of this package.

- 1- The package is essentially scalar. Cross -polar components cannot be obtained.
- 2- Offset geometries are treated using the projected aperture method.
- 3- The co-polar calculations of this package were impressive. This also applies to scattering from offset apertures. Only in extreme near field cases did the accuracy of the results (when compared with our benchmark GRASP) start to deteriorate.
- 4- The package is able to handle a wide range of optical components and sources.

2.4 GRASP (General Reflector and Antenna Software Package): The operation of GRASP is based on the well known “Physical Optics” method [4]. Physical Optics (PO) scattering calculations are performed in two main steps:

- 1 Calculate the equivalent currents induced on the scattering surface using the physical optics approximation.
- 2 Calculate the fields radiated by those currents using the “Equivalence Principle”.

To explain the principle of the PO approximation, consider first a plane wave illuminating a conducting surface. To calculate the currents at any point on the surface we attach a plane conductor tangent to the surface at that point. The induced equivalent electric and magnetic equivalent currents are given respectively by:

$$\mathbf{K} = \hat{\mathbf{n}} \times \mathbf{H}$$

$$\mathbf{K}^* = \mathbf{E} \times \hat{\mathbf{n}}$$

where \mathbf{E} and \mathbf{H} are the electric and magnetic fields respectively, and \mathbf{n} is a unit vector normal to the surface at the point of interest. The principle of the PO approximation is illustrated in Fig. 4.

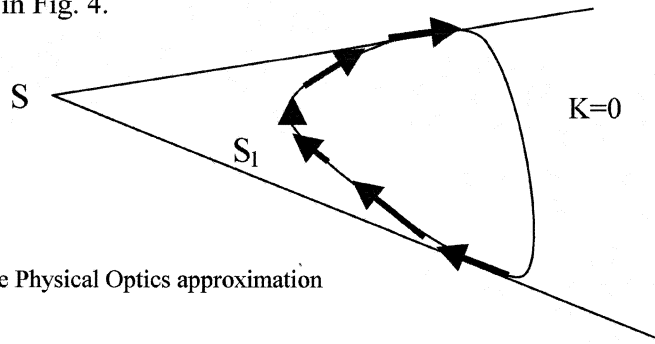


Figure 4 The Physical Optics approximation

Assume now that our scatterer is a perfect conductor illuminated by a point source. The induced currents in the PO approximation are found as follows. We made use of the fact that the tangential component of the electric field at the surface of a perfect conductor vanishes. Once the currents are known the corresponding vector potential can be calculated and subsequently the scattered fields, using the equivalence principle.

$$\mathbf{K}^{PO} = \begin{cases} \mathbf{n} \times \mathbf{H} = 2\mathbf{n} \times \mathbf{H}^i & \text{on } S_1 \\ 0 & \text{on the Shadow surface} \end{cases}$$

$$\mathbf{K}^{*PO} = 0 \quad \text{Everywhere}$$

The resultant electric field at a point a distance R from the origin is therefore given by

$$\mathbf{E} = \mathbf{E}^i - i\omega\mathbf{A} + \frac{\nabla\nabla \cdot \mathbf{A}}{i\omega\epsilon\mu}$$

$$\mathbf{A} = \frac{\mu}{4\pi} \oint_{S_1} \mathbf{K}^{PO} \frac{e^{ikR}}{R} dS$$

In the above equation \mathbf{E}^i is the incident field, \mathbf{A} is the vector potential and the integration is carried out over the illuminated surface of the scatterer. An equivalent expression could be written for the scattered magnetic field. At this stage two important aspects of this theory can be noticed:

- The PO approximation neglects the non-uniform currents near the edge of the scatterer. Our simulations however revealed that for practical aperture sizes, the effect of the non-uniform currents is only significant at very low levels (say below -40 db).
- Radiating the PO currents using GRASP is done rigorously according to Maxwell equations. No paraxial or scalar approximations are made. Both the electric and magnetic fields vectors are calculated.
- The information supplied by the output files of GRASP includes a full vector description of the scattered fields. All commonly required information (eg. co-polar and cross-polar components, spill-over, beam efficiency etc.) may be calculated using the information in the output files.
- GRASP takes care of the non-uniform edge-currents distribution using the “Physical Theory of Diffraction” (PTD) [5].

Our work in Phase I revealed that the PO method supplemented by the PTD correction yields solutions which are very close to the exact solutions of Maxwell equations. We arrived at this conclusion by comparing radiated fields simulated by GRASP using PO+PTD with those calculated by solving Maxwell equations using the method of moments. GRASP therefore was considered to be our benchmark for assessing results in Phase I. In Phase II of this project, we shall have the opportunity to compare the results simulated by GRASP with experimental results.

3. A Brief Discussion of Phase I Results

In what follows we shall present a summary of some important results from our work on Phase I. Some of these results are strongly related to the specific operation of the software packages but in many cases the results also reflect the nature of propagation and diffraction at submillimetre wavelengths. The following conclusions are related to scattering from single optical components illuminated by standard sources (point sources, plane wave, horns etc.).

- 1- Far field diffraction by an on-axis component: This is the simplest test case. All software packages, including ZEMAX, predicted the copolar component reasonably well.
- 2- Near field diffraction from an offset reflector: here we can distinguish between two cases. In the practical case where the diameter of the aperture was more than 10λ and the plane of observation was more than 30λ away, GRASP and GLAD gave consistently good and similar main beam patterns. On the other hand only GRASP was able to handle diffraction reasonably when the distance between the aperture and observation plane was further reduced. The quality of ASAP and CODE V depended on the particular test case, hence could not be considered reliable.
- 3- Most of the difficulties that software package encounter in producing accurate diffraction calculations result from their paraxial nature rather than neglecting edge effects in calculating an aperture distribution. The success of the physical optics method should not therefore be attributed to the way PO currents are calculated but rather to the rigorous way those currents are radiated.

- 4- Only GRASP output files gave the full vector behaviour of the scattered field. It was also the only package that produced reasonable low sidelobe levels below (say below -40 dB). Consequently, it was considered as a benchmark for Phase II.

We shall finish this section by two illustrative examples. The first concerning near field diffraction from a circular aperture illuminated by a plane wave.

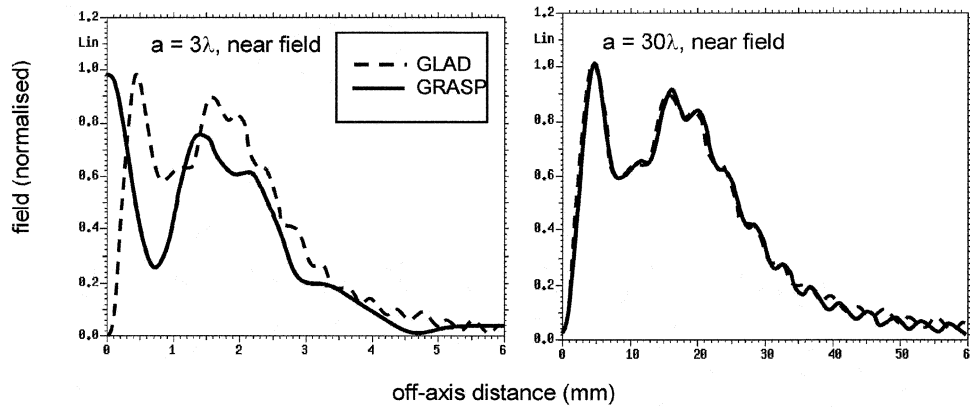


Figure 5 Beam amplitude in the near ($z_{\text{out}} = a^2/4\lambda$) field of an aperture of radius $a = 3\lambda$ and $a = 30\lambda$, calculated using GLAD and GRASP. GLAD is taken to be representative of the paraxial packages. $\lambda = 1$ mm in both cases.

Noticed that despite the extreme change in geometry between the two patterns above, all the paraxial packages did was simply to scale the pattern. The pattern predicted by GRASP however changed substantially. We in fact verified that this failure of the paraxial packages to predict the correct pattern has mainly resulted from incorrect prediction of the accurate longitudinal location of the Poisson spot.

The second example from Phase I is diffraction from an offset ellipsoid as shown in Fig. 6.

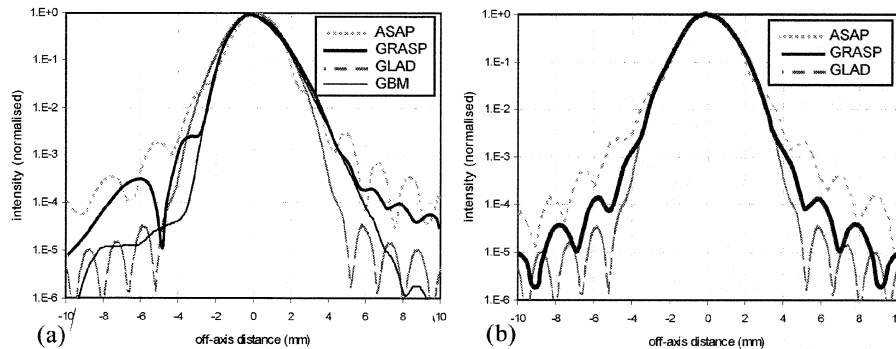


Figure 6 Intensity pattern at the output beam waist ($z_{\text{in}} = z_{\text{out}} = f = 12.57$ mm) for an ellipsoidal mirror of projected aperture $a = 1.5 \times W$. (a) shows a cut in the plane of asymmetry, (b) in the plane of symmetry. $\lambda = 1$ mm and $W_{\text{in}} = 2$ mm in both cases. The beams were calculated using ASAP, GLAD, GBM & GRASP.

Notice the failure of GLAD, ASAP, and GBM (Gaussian Beam Modes) to match the patterns predicted by GRASP, in particular in the plane of asymmetry. Substantial differences exist not only in the sidelobe level but also in the main beam. Notice that the failure of GLAD to perform well in this test case must be the result of the strong aberrations intrinsic to this system.

4. Analysis of HERSCHEL HIFI Channel

A description of a simplified version of channel I of HIFI of the ESA space telescope HERSCHEL (480-640 GHz) is shown in Fig. 7.

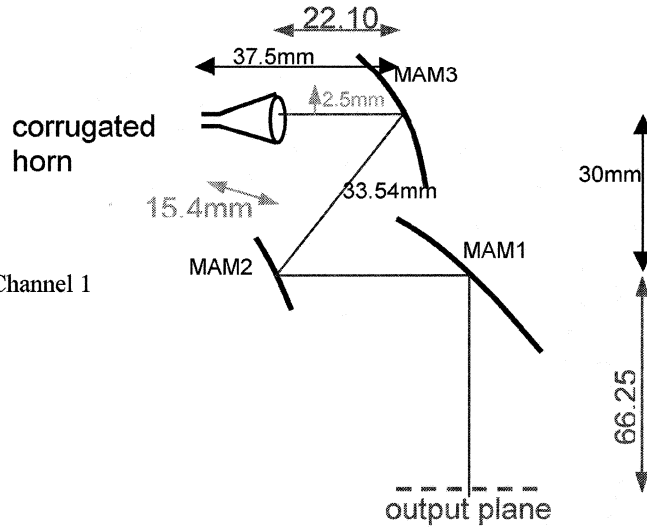


Figure 7 Layout of HIFI Channel 1

The system comprises a conical corrugated horn illuminating an off-axis ellipsoidal mirror. The beam is then focused onto a second ellipsoidal mirror before it is collimated by a 90 degrees offset parabolic reflector. Our plane of observation was located at the image of the telescope secondary mirror, 66.25 mm from the parabolic mirror MAM1. To emphasise the simulation differences between the packages, we carried out both focused simulations (0mm) and de-focused simulations by moving the horn aperture 5mm towards the mirror MAM3 (+5mm), 5 mm away from MAM3 (-5mm) and 10 mm away from MAM3 (-10). The projected aperture diameters of the mirrors MAM1, MAM2, MAM3 were respectively, 25 mm, 16 mm and 28 mm. In the following simulations the corrugated horn was assumed to support an ideal HE_{11} mode which can be written as

$$E(r) = E_0 J_0 \left(\frac{2.405}{a} r \right) e^{jk(\sqrt{R^2+r^2}-R)}$$

where R is the phase radius of curvature, a its radius and r is the radial coordinate of at the aperture. We have already shown a plot of the far field of this horn in Fig. 1. First we plotted both the symmetrical and asymmetrical cuts, at the output plane, when the horn was at the nominal focus. These are shown in Fig. 8

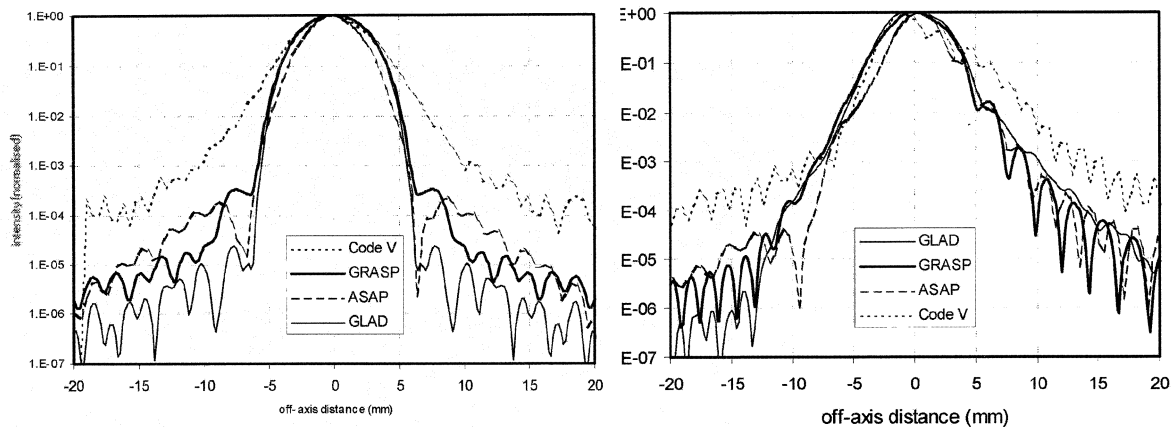


Figure 8 beam pattern predictions cuts in the plane of symmetry (left) and in the plane of asymmetry (right). The horn is at nominal focus.

Examining these results we notice that in the plane of symmetry, the agreement between GLAD and GRASP is good. ASAP does not do badly but the CODE V pattern is much wider than predicted by GRASP. The sidelobe level of GLAD seems too low, presumably as a result of under-estimating edge diffraction. A similar picture can be seen in the plane of asymmetry. Based on this we should already be able to see big differences in the measured results between CODE V and other packages. To enhance the predicted differences between GRASP and GLAD we carried out defocused simulations as shown in Fig. 9.

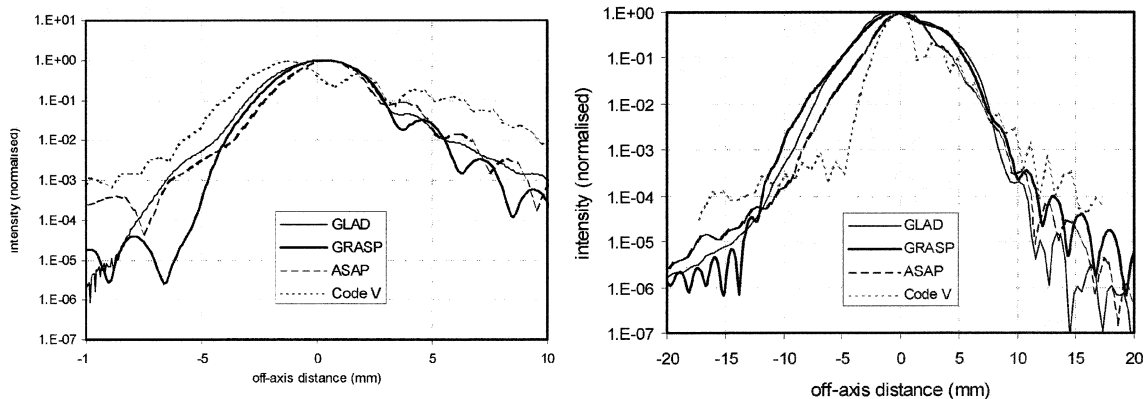


Figure 9 beam pattern predictions cuts in the plane of asymmetry. The horn is defocused by 5mm away from the mirror MAM3 (right) or towards the mirror (left).

It can be seen that the radiation pattern differences between the various packages have become substantial. To distinguish between ASAP, CODE V and GRASP experimentally we only require a dynamic range of -25 db. For GLAD we will need an amplitude dynamic range of about -30 db. For assessing GRASP against experimental measurement we are likely to require a dynamic range better than -40 db.

Finally, we also compared the phase simulations as shown in Fig. 10. The left hand plot represents measurements when the horn was at the focus and the right hand plot when the horn was moved 5 mm towards the mirrors. The phase differences between the various packages are substantial and our experimental system will easily be able to detect those differences.

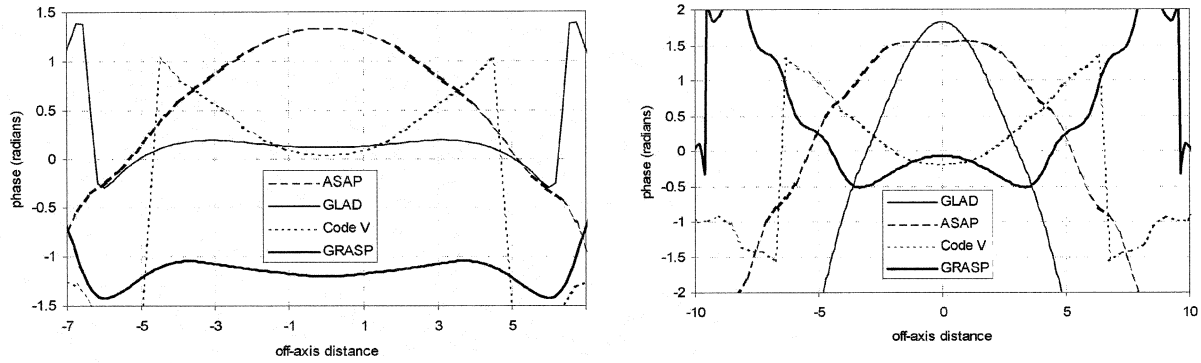


Figure 10 Main beam phase simulations (symmetric cut) when the horn is defocused by 5mm towards the mirror MAM3 (right) and at nominal focus (left).

5. The Near Field Detection System

We have already stated that a major theme of our work on phase II is the construction of a near field detection system which will allow us to measure the amplitude and phase of our patterns. Both the detection system and the test channel will be constructed at SRON and work is already at an advanced stage. A schematic diagram of the detection system is shown in Fig.11.

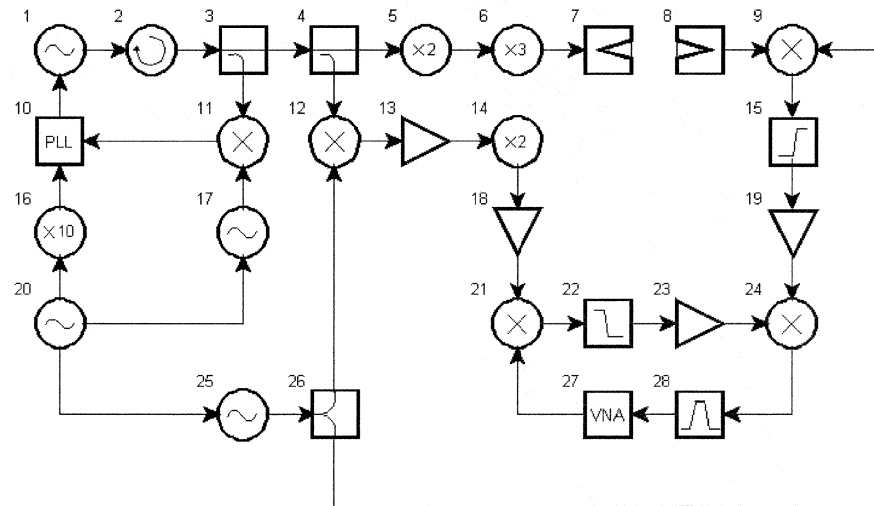


Fig. 11 The near field detection system

The detailed design of the 480 GHz near-field detection system (Fig. 11) was presented in the WP2-110 report.

Signal-to-noise calculations for the system gave a dynamic range of 33-55dB. 33dB was calculated for the worst case but the actual performance was expected to be better than this. The measured dynamic range (including also the coupling loss between the two horns, 7 & 8 in Fig. 11 was 40dB but the limitation was found to be a spurious

signal rather than the noise. We have already performed tests on the detection system by measuring the radiation pattern of the corrugated horn. Our preliminary results show indeed that we shall be able to obtain a dynamic range of -40 db. Together with phase measurements, the system will allow us to draw important conclusions regarding the quality of available commercial software for the analysis of submillimetre systems.

Acknowledgements

This work has been carried out as part of an ESA research contract (13043/98/NL/NB) Far IR Optics Design and Verification Tools'. The authors would like to acknowledge Peter de Maagt, Gert Ulbrich and Erico Armandillo of ESA for their useful comments.

References

1. Far-IR Optics Design and Verification Tools: Report on ESA research contract (13043/NL/NB).
2. O'Sullivan, C., *et al*: Far-Infrared Design & Verification, to appear in the July issue of Int. J. Infrared Millimetre Waves, 2002.
3. Jull, E. V.: Aperture Antennas and Diffraction Theory
4. Leo Diaz, : Antenna Engineering Using Physical Optics.
5. Shore, R.,A. and Yaghjian, A. D., : Incremental length diffraction coefficients for planar surface., IEEE Trans. Antenna and propagat. AP-36, pp. 55-70, 1988

